

Nucleon charge exchange on the deuteron: A critical review

François Lehar^{1,2} and Colin Wilkin³

¹ SPP IRFU, CEA Saclay, F-91190 Gif-sur-Yvette Cedex, France

² IEAP CTU, Horská 3a/22, Cz-12800 Prague 2, Czech Republic, e-mail: lehar@mail.utef.cvut.cz

³ Physics and Astronomy Department, UCL, Gower Street, London WC1E 6BT, United Kingdom, e-mail: cw@hep.ucl.ac.uk

Received: November 19, 2018

Abstract. The existing experimental data on the $d(n,p)nn$ and $d(p,n)pp$ cross sections in the forward direction are reviewed in terms of the Dean sum rule. It is shown that the measurement of the ratio of the charge exchange on the deuteron to that on the proton might, if taken together with other experimental data, allow a direct construction of the $np \rightarrow np$ scattering amplitude in the backward direction with few ambiguities.

PACS. 13.75.Cs Nucleon nucleon interactions – 25.40.Kv Charge-exchange reactions – 25.10.+s Nuclear reactions involving few-nucleon systems

1 Introduction

The nucleon-nucleon interaction is fundamental to the whole of nuclear physics and hence to the composition of matter as we know it. Apart from its intrinsic importance, it is also a necessary ingredient in the description of meson production and other intermediate energy processes.

In the case of proton-proton scattering, the data set of differential and total cross sections and the various single and multi-spin observables is very extensive and this has allowed the construction of reliable isospin $I = 1$ phase shifts up to at least 2 GeV [1]. The situation is far less developed for the isoscalar $I = 0$ case, where the corresponding phase shift analysis is only available up to 1.3 GeV and even then there are significant ambiguities at the higher energies [1].

More good data on neutron-proton scattering are clearly needed, possibly with the aim of directly reconstructing the isosinglet amplitudes. This is particularly promising in the forward direction [2] but the conditions are almost as favourable for backward $pn \rightarrow np$ scattering (often loosely called the np charge-exchange region) and it is this which we want to consider in some detail in this paper.

To avoid some of the problems associated with the quality of neutron beams and/or the detection of neutron, the deuteron is often used successfully as a substitute target or beam. For example, it has been shown that the spin correlation and transfer parameters in pp quasi-elastic scattering in the 1.1 to 2.4 GeV range are very close to those measured in free pp collisions [3] and the Saclay group find exactly the same reassurance for pn quasi-elastic scattering [4].

One particular valuable tool that can be used to study the backward amplitudes is the comparison of the quasi-

free (p,n) or (n,p) reaction on the deuteron to the free backward elastic scattering on a nucleon target. It was emphasised over 50 years ago that the reaction on the deuteron can act, in suitable kinematic regions, as a spin filter that selects the spin-dependent contribution to the np elastic cross section [5]. This sensitivity arises from the Pauli principle, which blocks any spin-1 component in the low energy $\{nn\}$ or $\{pp\}$ system. To avoid the explicit introduction of the dynamics of the low energy NN system, Dean [6] derived a sum rule for the ratio R_{np} of the differential cross section for charge exchange on the deuteron to that on the nucleon. Although this is given as a function of the momentum transfer q , it simplifies for collinear dynamics to the extent that there is then no dependence on the deuteron structure. More importantly, the sum rule converges very fast as a function of the excitation energy for small q , due to the strength of the low energy 1S_0 NN interaction. It has therefore been used in the analysis of the wealth of R_{np} data, which now extend up to 2 GeV [7]. It is the aim of the present paper to show how such data, combined with other measurements, might contribute to an analysis of the elastic neutron-proton scattering amplitudes in the backward direction.

In section 2 we summarise the amplitudes and some observables that are relevant for backward elastic np scattering. Of particular importance in this context is the fact that the conventional NN amplitudes ¹ are not the most suitable ones when analysing charge exchange on the deuteron, where it is necessary to take into account of the interchange between the final neutron and proton *ab initio*. The impulse approximation dynamics and the form of

¹ See Ref. [8] for a very comprehensive discussion of different amplitude bases.

the Dean sum rule in the forward direction are described in section 3, where some of the underlying assumptions are clarified. It is shown there that the sum rule saturates very quickly, which make it such a useful tool.

Section 4 gives an extensive compilation of the values of $R_{np}(0)$ derived from the $nd \rightarrow p\{nn\}$, $pd \rightarrow n\{pp\}$, and $dp \rightarrow \{pp\}n$ reactions and it is shown there that the total error bars are the smallest in the (n, p) case provided that a good quality neutron beam is available. On the basis of the existing phase shift analysis [1], impulse approximation predictions of $R_{np}(0)$ can be made up to a beam energy of 1.3 GeV and the agreement with experimental data is very reasonable down to at least 300 MeV. However, it is important to reiterate that values of $R_{np}(0)$ are now available up to 2 GeV. The prospects for a $np \rightarrow np$ elastic amplitude reconstruction in the backward direction are discussed in the conclusions of section 5, where it is shown that, with extra information available through the use of polarised deuterons, this is now becoming feasible.

2 Neutron-proton amplitudes and observables

The nucleon-nucleon formalism, including the four-index notation and definition of all *pure* experiments, is discussed in full detail in Ref. [8]. In this work the matrix describing elastic neutron-proton scattering is written in the form

$$\begin{aligned} M(\mathbf{k}_f, \mathbf{k}_i) = & \frac{1}{2}[(a+b) + (a-b)(\boldsymbol{\sigma}_n \cdot \hat{\mathbf{n}})(\boldsymbol{\sigma}_p \cdot \hat{\mathbf{n}}) \\ & + (c+d)(\boldsymbol{\sigma}_n \cdot \hat{\mathbf{m}})(\boldsymbol{\sigma}_p \cdot \hat{\mathbf{m}}) + (c-d)(\boldsymbol{\sigma}_n \cdot \hat{\boldsymbol{\ell}})(\boldsymbol{\sigma}_p \cdot \hat{\boldsymbol{\ell}}) \\ & + e(\boldsymbol{\sigma}_n + \boldsymbol{\sigma}_p) \cdot \hat{\mathbf{n}}], \end{aligned} \quad (2.1)$$

where a, b, c, d and e are complex invariant amplitudes, which are functions of energy and scattering angle θ . The 2×2 Pauli matrices $\boldsymbol{\sigma}_n$ and $\boldsymbol{\sigma}_p$ act in the spaces of the proton and neutron spins, respectively.

In terms of the c.m. momenta in the initial and final states, \mathbf{k}_i and \mathbf{k}_f , an orthonormal basis system is defined through

$$\hat{\mathbf{n}} = \frac{\mathbf{k}_i \times \mathbf{k}_f}{|\mathbf{k}_i \times \mathbf{k}_f|}, \quad \hat{\boldsymbol{\ell}} = \frac{\mathbf{k}_f + \mathbf{k}_i}{|\mathbf{k}_f + \mathbf{k}_i|}, \quad \hat{\mathbf{m}} = \frac{\mathbf{k}_f - \mathbf{k}_i}{|\mathbf{k}_f - \mathbf{k}_i|}, \quad (2.2)$$

which satisfy $\hat{\mathbf{m}} = \hat{\mathbf{n}} \times \hat{\boldsymbol{\ell}}$.

For later purposes, it is convenient to choose the invariant normalisation, where the unpolarised cross section is given by

$$\left(\frac{d\sigma}{dt}\right)_{np \rightarrow np} = \frac{1}{2}(|a|^2 + |b|^2 + |c|^2 + |d|^2 + |e|^2), \quad (2.3)$$

where t is the four-momentum transfer between the initial and final neutrons.

In the forward direction $e = 0$ and, since one can then not distinguish between the two perpendicular axes, $a(0) - b(0) = c(0) + d(0)$. The scattering matrix then reduces to

$$\begin{aligned} M(\mathbf{k}_i, \mathbf{k}_i) = & \frac{1}{2}[(a(0) + b(0)) + (c(0) - d(0))(\boldsymbol{\sigma}_n \cdot \hat{\boldsymbol{\ell}})(\boldsymbol{\sigma}_p \cdot \hat{\boldsymbol{\ell}}) \\ & + (a(0) - b(0))\{(\boldsymbol{\sigma}_n \cdot \hat{\mathbf{n}})(\boldsymbol{\sigma}_p \cdot \hat{\mathbf{n}}) + (\boldsymbol{\sigma}_n \cdot \hat{\mathbf{m}})(\boldsymbol{\sigma}_p \cdot \hat{\mathbf{m}})\}] \end{aligned} \quad (2.4)$$

There are three spin-correlated total cross sections defined by

$$\sigma_{\text{tot}} = \sigma_0 - \frac{1}{2}\Delta\sigma_L \mathcal{P}_n^L \mathcal{P}_p^L - \frac{1}{2}\Delta\sigma_T \boldsymbol{\mathcal{P}}_n^T \cdot \boldsymbol{\mathcal{P}}_p^T, \quad (2.5)$$

where \mathcal{P}^L and $\boldsymbol{\mathcal{P}}^T$ are the longitudinal and transverse components of the polarisation of either the initial neutron or proton.

The imaginary parts of the three independent forward amplitudes can be determined through measurements of these total cross sections using the relations:

$$\begin{aligned} \sigma_0 &= 2\sqrt{\pi} \text{Im}[a(0) + b(0)], \\ -\Delta\sigma_T &= 4\sqrt{\pi} \text{Im}[a(0) - b(0)], \\ -\Delta\sigma_L &= 4\sqrt{\pi} \text{Im}[c(0) - d(0)]. \end{aligned} \quad (2.6)$$

We are interested in backward rather than forward neutron-proton scattering, in a region that is often called neutron-proton charge exchange. The interchange of the momenta of the final neutron and proton is achieved by letting $\mathbf{k}_f \rightarrow -\mathbf{k}_f$ and, as is seen from Eq.(2.2), this introduces a new set of basis vectors, which are related to the original ones through

$$\hat{\mathbf{n}}_{ce} = -\hat{\mathbf{n}}, \quad \hat{\boldsymbol{\ell}}_{ce} = -\hat{\mathbf{m}}, \quad \hat{\mathbf{m}}_{ce} = -\hat{\boldsymbol{\ell}}. \quad (2.7)$$

The scattering matrix in this representation becomes

$$\begin{aligned} M(-\mathbf{k}_f, \mathbf{k}_i) = & \frac{1}{2}[(a+b) + (a-b)(\boldsymbol{\sigma}_n \cdot \hat{\mathbf{n}}_{ce})(\boldsymbol{\sigma}_p \cdot \hat{\mathbf{n}}_{ce}) \\ & + (c+d)(\boldsymbol{\sigma}_n \cdot \hat{\boldsymbol{\ell}}_{ce})(\boldsymbol{\sigma}_p \cdot \hat{\boldsymbol{\ell}}_{ce}) + (c-d)(\boldsymbol{\sigma}_n \cdot \hat{\mathbf{m}}_{ce})(\boldsymbol{\sigma}_p \cdot \hat{\mathbf{m}}_{ce}) \\ & - e(\boldsymbol{\sigma}_n + \boldsymbol{\sigma}_p) \cdot \hat{\mathbf{n}}_{ce}], \end{aligned} \quad (2.8)$$

which, in the strictly backward direction of $\theta = \pi$, reduces to

$$\begin{aligned} M(-\mathbf{k}_i, \mathbf{k}_i) = & \frac{1}{2}[(a(\pi) + b(\pi)) + \\ & (c(\pi) + d(\pi))(\boldsymbol{\sigma}_n \cdot \hat{\boldsymbol{\ell}}_{ce})(\boldsymbol{\sigma}_p \cdot \hat{\boldsymbol{\ell}}_{ce}) + \\ & (a(\pi) - b(\pi))\{(\boldsymbol{\sigma}_n \cdot \hat{\mathbf{n}}_{ce})(\boldsymbol{\sigma}_p \cdot \hat{\mathbf{n}}_{ce}) \\ & + (\boldsymbol{\sigma}_n \cdot \hat{\mathbf{m}}_{ce})(\boldsymbol{\sigma}_p \cdot \hat{\mathbf{m}}_{ce})\}], \end{aligned} \quad (2.9)$$

where $e(\pi) = 0$ and $a(\pi) - b(\pi) = c(\pi) - d(\pi)$.

If one invokes the symmetry properties of the amplitudes that follow from isospin invariance [8], the backward values of the imaginary parts of the three independent amplitudes are, in principle, determined by the values of the spin-dependent total cross sections for neutron-proton and proton-proton scattering:

$$\begin{aligned} \text{Im}[a(\pi)] &= \frac{1}{8\sqrt{\pi}} \left(2\sigma_0^{(-)} - \Delta\sigma_T^{(-)}\right), \\ \text{Im}[b(\pi)] &= \frac{1}{8\sqrt{\pi}} \left(\Delta\sigma_T^{(-)} + \Delta\sigma_L^{(-)}\right), \\ \text{Im}[c(\pi)] &= \frac{1}{8\sqrt{\pi}} \left(2\sigma_0^{(-)} + \Delta\sigma_T^{(-)}\right), \\ \text{Im}[d(\pi)] &= -\frac{1}{8\sqrt{\pi}} \left(\Delta\sigma_T^{(-)} - \Delta\sigma_L^{(-)}\right), \end{aligned} \quad (2.10)$$

where we use the notation

$$\sigma^{(-)} \equiv \sigma(np) - \sigma(pp) \quad (2.11)$$

for all three total cross sections.

However, in the theoretical treatment of the charge exchange on the deuteron, *i.e.* $nd \rightarrow p\{nn\}$ at small angles between the incident neutron and final proton, it is convenient to work with an alternative amplitude decomposition [9]:

$$\begin{aligned} M^{ce}(\mathbf{k}_f, \mathbf{k}_i) = & \mathcal{P}_{p \leftrightarrow n} [\alpha^{ce} + i\gamma^{ce}(\boldsymbol{\sigma}_n + \boldsymbol{\sigma}_p) \cdot \hat{\mathbf{n}}_{ce} \\ & + \beta^{ce}(\boldsymbol{\sigma}_n \cdot \hat{\mathbf{n}}_{ce})(\boldsymbol{\sigma}_p \cdot \hat{\mathbf{n}}_{ce}) + \delta^{ce}(\boldsymbol{\sigma}_n \cdot \hat{\mathbf{m}}_{ce})(\boldsymbol{\sigma}_p \cdot \hat{\mathbf{m}}_{ce}) \\ & + \epsilon(\boldsymbol{\sigma}_n \cdot \hat{\boldsymbol{\ell}}_{ce})(\boldsymbol{\sigma}_p \cdot \hat{\boldsymbol{\ell}}_{ce})], \end{aligned} \quad (2.12)$$

where the operator $\mathcal{P}_{p \leftrightarrow n}$ interchanges the charge labels on the final proton and neutron. The presence of this operator means that α^{ce} represents the spin-independent amplitude between the initial neutron and final proton whereas the $(a + b)$ of Eq. (2.1) corresponds to the spin-independent amplitude between the initial and final neutrons.

It is straightforward to find the relationship between these two representations and, for the collinear situation that is of interest to us here, we have

$$\begin{aligned} \alpha^{ce}(0) &= \frac{1}{2} (a(\pi) + c(\pi)) , \\ \beta^{ce}(0) &= \delta^{ce}(0) = \frac{1}{2} (a(\pi) - c(\pi)) , \\ \epsilon^{ce}(0) &= \frac{1}{2} (b(\pi) + d(\pi)) . \end{aligned} \quad (2.13)$$

The relation between the imaginary parts of these forward amplitudes and the total cross sections is more intuitively obvious:

$$\begin{aligned} \text{Im}[\alpha^{ce}(0)] &= \frac{1}{4\sqrt{\pi}} \sigma_0^{(-)} , \\ \text{Im}[\beta^{ce}(0)] &= -\frac{1}{8\sqrt{\pi}} \Delta\sigma_T^{(-)} , \\ \text{Im}[\epsilon^{ce}(0)] &= \frac{1}{8\sqrt{\pi}} \Delta\sigma_L^{(-)} . \end{aligned} \quad (2.14)$$

Extra information on the real parts of these amplitudes might be obtained through the use of forward dispersion relations. This is likely to be of most value for the spin-independent term, which only involves unpolarised total cross section input. However, this approach will not be pursued here.

From the relations given in Ref. [8], the magnitudes of these charge-exchange amplitudes in the forward direction are given in terms of the backward elastic np differential cross section and spin-transfer parameters K_{0nn0} and K_{0l0} through

$$\begin{aligned} |\alpha^{ce}(0)|^2 &= \frac{1}{4} [1 + 2K_{0nn0}(\pi) + K_{0l0}(\pi)] \left(\frac{d\sigma}{dt} \right)_{np \rightarrow np} , \\ |\beta^{ce}(0)|^2 &= \frac{1}{4} [1 - K_{0l0}(\pi)] \left(\frac{d\sigma}{dt} \right)_{np \rightarrow np} , \\ |\epsilon^{ce}(0)|^2 &= \frac{1}{4} [1 - 2K_{0nn0}(\pi) + K_{0l0}(\pi)] \left(\frac{d\sigma}{dt} \right)_{np \rightarrow np} \end{aligned} \quad (2.15)$$

It should be noted that the corresponding results for the non-charge-exchange amplitudes, *i.e.* without the interchange operator $\mathcal{P}_{p \leftrightarrow n}$ in Eq. (2.12), have a similar structure but with the K being replaced by the depolarisation

parameters D . This arises because of the different assignment of the labels *scattered* and *recoil* to the final particles in the two decompositions. Of course, the *elastic* and *charge-exchange* representations must lead to the same physics for elastic neutron-proton scattering, with merely interpretational differences.

Using the above relations in association with the phase shift predictions from the SAID database [1], one sees that the spin-independent term $|\alpha^{ce}(0)|^2$ should contribute less than 10% to the forward charge-exchange cross section between say 200 MeV up to the limit of the SAID analysis at 1.3 GeV. In contrast, there is relatively little spin flip between the initial and final neutrons, *i.e.* the $|a(\pi) + b(\pi)|^2$ term dominates. One has therefore to be very careful to specify clearly the meaning of any statement comparing the magnitudes of the spin-flip and spin-independent contributions in backward neutron-proton elastic scattering.

3 Charge exchange on the deuteron

In single-scattering (impulse) approximation, the charge exchange $nd \rightarrow p\{nn\}$ reaction on the deuteron is thought of as a $np \rightarrow pn$ reaction with a spectator neutron². Initially the neutron-proton pair is bound in the deuteron and the two emerging neutrons are subject to a final state interaction, as illustrated diagrammatically in Fig. 1. If \mathbf{k} , the relative momentum in the nn system, and hence the excitation energy $E_{nn} = k^2/m$, are small, the final neutrons are in the 1S_0 state. The reaction therefore acts as a spin-isospin filter going from the $({}^3S_1, {}^3D_1)$ of the deuteron to the final 1S_0 of the dineutron. Furthermore, at low momentum transfers $\mathbf{q} = \mathbf{k}_f - \mathbf{k}_i$ between the initial neutron and final proton other final states are only weakly excited. Under such conditions the $nd \rightarrow p\{nn\}$ differential cross section depends but weakly upon the spin-independent amplitude α^{ce} of Eq. (2.12).

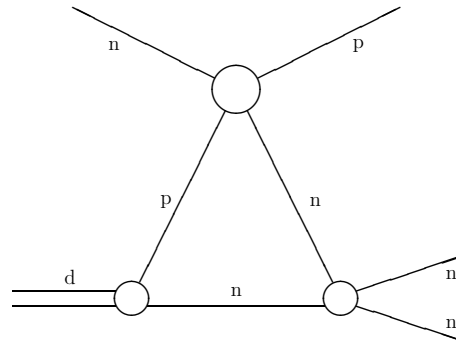


Fig. 1. Impulse approximation diagram for nucleon charge exchange on the deuteron.

The above features were put on a simple quantitative basis through the use of a sum rule by Dean [6] and

² Since the deuteron has isospin-zero, the description of the $pd \rightarrow n\{pp\}$ reaction is formally identical.

this was extended to polarisation observables by Bugg and Wilkin [9]. The matrix element of the transition is of the form [10]

$$\mathcal{F}(\mathbf{k}_f, \mathbf{k}_i; S, \nu_f, M, m_p, m_n) = \langle \Psi_{nn, \mathbf{k}}^{(-)}; S, \nu_f, m_p | M^{ce}(\mathbf{k}_f, \mathbf{k}_i) \exp(\frac{1}{2}i\mathbf{q} \cdot \mathbf{r}) | \Phi_d^M, m_n \rangle, \quad (3.1)$$

where $\Phi_d(\mathbf{r})$ is the deuteron wave function in configuration space and $\Psi_{nn, \mathbf{k}}^{(-)}$ the corresponding for the low energy nn final state of spin S and projection ν_f . The magnetic quantum numbers of the initial neutron and deuteron and the final proton are denoted by m_n , M , and m_p , respectively.

The unpolarised cross section is normalised such that

$$\frac{d4\sigma}{dt d^3k} = \frac{1}{6} \text{Tr} \{ \mathcal{F}^\dagger \mathcal{F} \}, \quad (3.2)$$

where the trace is over all the spin projections.

Dean noted that, if one summed Eq. (3.2) over all excitation energies of the dineutron, one could obtain a sum rule that did not depend upon the details of the low energy nn interaction. This is a high energy approximation and, for it to be valid, the available phase space must be so large as not to disturb the convergence of the sum rule, as discussed below.

Specialising to the case of interest here, *viz.*, $\theta_{np} = 0^\circ$, $q \approx 0$, the sum rule for the differential cross section reduces to

$$\begin{aligned} \frac{d\sigma}{dt}(nd \rightarrow p\{nn\}) &= \int \frac{d^4\sigma}{dt} d^3k \\ &= \frac{2}{3} (2|\beta^{ce}(0)|^2 + |\epsilon^{ce}(0)|^2). \end{aligned} \quad (3.3)$$

For completeness, we give also the corresponding sum rule for the deuteron tensor analysing power t_{20} ;

$$\begin{aligned} t_{20} \frac{d\sigma}{dt}(nd \rightarrow p\{nn\}) \\ = \frac{2\sqrt{2}}{3} (1 - \frac{9}{10}P_D) (|\beta^{ce}(0)|^2 - |\epsilon^{ce}(0)|^2), \end{aligned} \quad (3.4)$$

where P_D is the deuteron D -state probability.

The Dean sum rule may then be written in terms of $np \rightarrow np$ elastic scattering observables as

$$\begin{aligned} R_{np}(0) &= \frac{d\sigma(nd \rightarrow p\{nn\})/dt}{d\sigma(np \rightarrow pn)/dt} \Big|_{q=0} \\ &= \frac{2}{3} \frac{2|\beta^{ce}(0)|^2 + |\epsilon^{ce}(0)|^2}{|\alpha^{ce}(0)|^2 + 2|\beta^{ce}(0)|^2 + |\epsilon^{ce}(0)|^2} \\ &= \frac{1}{6} [3 - K_{000}(\pi) - 2K_{0nn0}(\pi)]. \end{aligned} \quad (3.5)$$

The sum rule of Eq. (3.5) is very effective at medium and high energies because it converges so quickly. This is illustrated in Fig. 2, where the impulse approximation cross section of Eq. (3.2) has been evaluated for the $pd \rightarrow n\{pp\}$ case [10] and integrated numerically over the pp excitation energy. Although a specific nucleon-nucleon potential was used [11], the rate of convergence depends little

upon this choice and less than 1% of the sum rule remains beyond $E_{pp} \approx 15$ MeV. The rate of convergence under the specific conditions of the Dubna $d(n, p)nn$ experiment [7] has also been discussed by Ladygina [12].

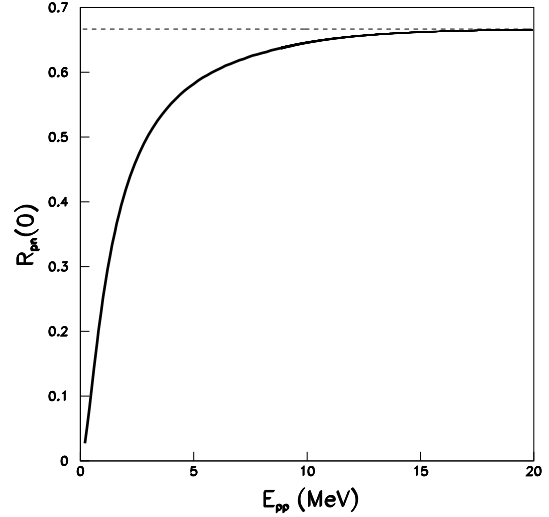


Fig. 2. Convergence of the sum rule for the $pd \rightarrow n\{pp\}$ reaction at $q = 0$ as a function of the excitation energy in the final pp system. It has been assumed that the spin-non-flip amplitude $\alpha^{ce} = 0$ to make the limiting value $\frac{2}{3}$, though the rate of convergence is similar in all cases. The evaluation has been carried out using the de Toureill and Sprung potential [11] to describe the low energy nucleon-nucleon systems, as explained in Ref. [10].

Deviations might be expected from the sum rule at lower energies where the phase space available does not allow an unimpeded integration over E_{nn} . As discussed in section 4, this has only a marginal effect on the saturation of the sum rule for incident energies above 50 MeV. More critical, though, is the fact that at low energies experimentalists generally put a more severe cut on the momentum of the final proton in the $nd \rightarrow p\{nn\}$ reaction to minimise the contributions from diagrams other than those of the impulse approximation and this reduces the value obtained for $R_{np}(0)$. Although we later report results at low energies, there is no reason to believe that the impulse approximation of Fig. 1 should dominate there and a full three-body calculation has to be undertaken to interpret these results.

The most significant correction to the sum rule at high energies comes from the shadow effect [13], which will typically reduce the value of $R_{np}(0)$ by about 5%.

Table 1. Summary of the available experimental data on the $R_{np}(0)$ ratio measured using the $nd \rightarrow p\{nn\}$ reaction. The error bars reflect both the statistical and systematic uncertainties.

T_{kin} (MeV)	$R_{np}(0)$	Year	Ref.
13.9	0.185	1965	[14]
90.0	0.397 ± 0.044	1951	[15]
152.0	0.650 ± 0.100	1966	[16]
200.0	0.553 ± 0.030	1962	[17]
270.0	0.710 ± 0.021	1952	[18]
299.7	0.652 ± 0.033	1988	[19]
319.8	0.643 ± 0.032	1988	[19]
339.7	0.637 ± 0.032	1988	[19]
359.6	0.626 ± 0.031	1988	[19]
379.6	0.641 ± 0.032	1988	[19]
380.0	0.200 ± 0.035	1955	[20]
399.7	0.610 ± 0.031	1988	[19]
419.8	0.623 ± 0.031	1988	[19]
440.0	0.630 ± 0.032	1988	[19]
460.1	0.611 ± 0.031	1988	[19]
480.4	0.608 ± 0.030	1988	[19]
500.9	0.592 ± 0.030	1988	[19]
521.1	0.604 ± 0.030	1988	[19]
539.4	0.617 ± 0.031	1988	[19]
550.0	0.589 ± 0.046	2007	[7]
557.4	0.632 ± 0.032	1988	[19]
710.0	0.483 ± 0.080	1960	[21]
794.0	0.560 ± 0.040	1978	[22]
800.0	0.554 ± 0.023	2007	[7]
1000	0.553 ± 0.026	2007	[7]
1200	0.551 ± 0.022	2007	[7]
1400	0.576 ± 0.038	2007	[7]
1800	0.568 ± 0.033	2007	[7]
2000	0.564 ± 0.045	2007	[7]

4 Experimental data and theoretical comparison

The cross section ratio $R_{np}(0)$ can be investigated using either the $nd \rightarrow p\{nn\}$, $pd \rightarrow n\{pp\}$, or the $dp \rightarrow \{pp\}n$ reaction and the experimental results in the three cases are summarised, respectively, in Tables 1, 2, and 3. In many cases the results had to be read from graphs and this is especially true of some of the very old data. However, because of their age, such data tend to be at the lower energies, which are of less interest for the amplitude reconstruction.

There are more measurements of the $nd \rightarrow p\{nn\}$ reaction than of $pd \rightarrow n\{pp\}$ and the error bars are also generally smaller. This reflects the relative difficulty in the two types of experiment. If a good quality neutron beam is available, the measurement of the relative strengths of the proton spectra from deuterium and hydrogen targets is comparatively *straightforward*. The alternative of measuring the neutron in the final state presents far more difficulties. The third technique of using a deuteron beam has only been attempted once because in this case one has

Table 2. Summary of the available experimental data on the $R_{np}(0)$ ratio measured using the $pd \rightarrow n\{pp\}$ reaction. The error bars reflect both the statistical and systematic uncertainties.

T_{kin} (MeV)	$R_{np}(0)$	Year	Ref.
13.5	0.180	1959	[23]
30.1	0.141 ± 0.035	1967	[24]
50.0	0.240 ± 0.060	1967	[24]
95.0	0.480 ± 0.030	1953	[25]
95.7	0.587 ± 0.029	1967	[26]
135.0	0.652 ± 0.154	1965	[27]
143.9	0.601 ± 0.057	1967	[26]
647.0	0.600 ± 0.080	1976	[28]
800.0	0.660 ± 0.080	1976	[28]

Table 3. Summary of the available experimental data on the $R_{np}(0)$ ratio measured using the $dp \rightarrow \{pp\}n$ reaction. The kinetic energy quoted here is the energy per nucleon. The error bars reflect both the statistical and systematic uncertainties.

T_{kin} (MeV)	$R_{np}(0)$	Year	Ref.
977.0	0.430 ± 0.220	1975	[29]
977.0	0.650 ± 0.120	2002	[30]

to measure both final fast protons over a large range of phase space. This can be done using a bubble chamber and the value [30] quoted in Table 3 represents the result of increased statistics and a different analysis compared to that of the previous publication [29]. A particular criticism here is that the free neutron-proton data have to be taken from an entirely different source so that there can be no cancellations between any systematic errors.

Although, as shown by Fig. 2, the sum rule converges quite fast, there is nevertheless a problem at low energies as to where to cut the tail in the proton spectrum and, in certain cases, it is likely that the choice has not allowed for a full saturation of the sum rule.

The different measurements of $R_{np}(0)$ are reported in Fig. 3 with one controversial point [20] being omitted. Also shown are the estimates of Eq. (3.5), evaluated using the current SAID solution [1]. In these predictions, no account has been taken of the shadow effect [13], which would reduce the limiting value to typically 0.63/0.64. The agreement with the phase shift predictions is generally satisfactory, though there are suggestions from the new data [7] that there might be some underestimate of the relative strength of the $|\alpha^{ce}(0)|^2$ contribution at the higher energies.

At low energies the predictions fall steeply. In part this is related to the behaviour of the np amplitudes but one has also to take account of the fact that the smaller available phase space does not allow the sum rule to be fully

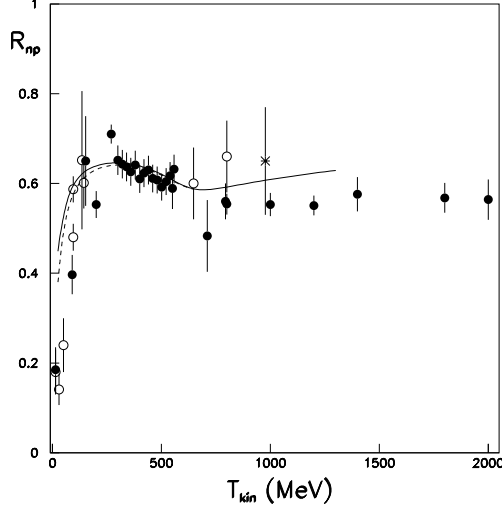


Fig. 3. Experimental data on the $R_{np}(0)$ ratio at zero momentum transfer. The closed circles are from the (n, p) data of Table 1, the open circles from the (p, n) data of Table 2, and the cross from the $(d, 2p)$ datum of Table 3. These results are compared to the Dean sum-rule predictions of Eq. (3.5) using the current SAID solution, which is available up to a laboratory kinetic energy of 1.3 GeV. The dashed curve takes into account the limited phase space available at the lower energies.

saturated. However, even when this effect is included, by integrating numerically the impulse approximation, the effect is comparatively small and does not account for the much steeper drop in the experimental data. Of much more importance there is the experimental cut in the recoil proton momentum and, of course, the deviations from the naive impulse approximation at low energies.

5 Summary and conclusions

The ratio $R_{np}(0)$ of the forward differential cross section for charge exchange on the deuteron to that on the nucleon is a very robust observable since many uncertainties drop out between the two measurements. It is therefore not surprising that one gets a consistent picture of the energy dependence of this quantity from measurements of the $nd \rightarrow p\{nn\}$, $pd \rightarrow n\{pp\}$, and $dp \rightarrow \{pp\}n$ reactions. Furthermore, we have shown that, from about 300 MeV up to 1.3 GeV, where the np phase shift analyses terminate, the predictions for $R_{np}(0)$ largely agree with the available experimental data. Since measurements of $R_{np}(0)$ have now been carried out up to 2 GeV [7], it is appropriate to consider whether a neutron-proton elastic amplitude reconstruction could be performed using these results.

In the backward direction, we see from Eq. (2.13) that there are only three (complex) amplitudes, $\alpha^{ce}(0)$, $\beta^{ce}(0)$, and $\epsilon^{ce}(0)$. In principle, as shown by Eq. (2.14), the imaginary parts of these amplitudes can be fixed by measurements of the spin dependence of the pp and np total cross

sections. According to the available phase shift analyses, these quantities are much smaller than the real parts and so the error bars will be relatively large, even if all the measurements were available. The values of $|\alpha^{ce}(0)|^2$ and $2|\beta^{ce}(0)|^2 + |\epsilon^{ce}(0)|^2$ would be fixed by the combined measurement of $R_{np}(0)$ and the free $np \rightarrow np$ differential cross section.

Measurements have been carried out on the t_{20} tensor analysing power of the $\vec{d}p \rightarrow \{pp\}n$ reaction [31, 32, 33]. Rather than using the sum rule of Eq. (3.4), these data were taken with an excitation energy in the pp system so low that the final 1S_0 system dominates or where one could correct from contamination for the pp P -waves. Under such conditions,

$$t_{20} = \sqrt{2} \left(\frac{|\beta^{ce}(0)|^2 - |\epsilon^{ce}(0)|^2}{2|\beta^{ce}(0)|^2 + |\epsilon^{ce}(0)|^2} \right). \quad (5.1)$$

Furthermore, a measurement of the transverse spin correlation with an incident vector polarised deuteron on a polarised hydrogen target would give [34]

$$C_{n,n}(0) = \frac{-2\text{Re}(\beta^{ce}(0)^* \epsilon^{ce}(0))}{2|\beta^{ce}(0)|^2 + |\epsilon^{ce}(0)|^2}. \quad (5.2)$$

It is therefore clear that, even with very good data on these seven parameters, there would still be two discrete ambiguities, *viz.* the signs of the $\text{Re}(\alpha^{ce}(0))$ and $\text{Re}(\beta^{ce}(0))$. However, since there are extensive data on the unpolarised cross section difference of Eq. (2.14), the application of forward dispersion relations will certainly be sufficient to determine at least the sign of $\text{Re}(\alpha^{ce}(0))$. Regarding the other ambiguity, if $\text{Re}(\beta^{ce}(0))$ changes sign then this would be reflected in the value of $t_{20}(0)$, which has been found to have the same sign throughout the measured range [31, 32, 33]. In principle, therefore, it seems that a direct amplitude construction of $np \rightarrow np$ in the backward direction is feasible without having to measure differential cross sections with polarised protons and neutrons, although these would clearly enhance the precision of any analysis.

For obvious experimental reasons, the measurements of deuteron charge exchange leading to the low excitation energy pp system have so far been carried out with a polarised deuteron beam [31, 32, 33]. This lowers the limit on the energy per nucleon. However, a polarised hydrogen/deuterium gas target is now available at the ANKE facility of the COSY-Jülich storage ring [35]. Using solid state telescopes placed within the target chamber, the low energy protons from the $\vec{p}\vec{d} \rightarrow n\{pp\}$ reaction can be measured with high precision. This will allow the values of $t_{20}(0)$ and $C_{n,n}(0)$ to be investigated up to the maximum proton beam energy of 2.9 GeV.

This work has resulted from an active and productive collaboration with the Dubna DELTA-SIGMA group of Ref. [7], for which we are very appreciative. We are also grateful to J. Ludwig for furnishing us with a copy of Ref. [19]. One of the authors (CW) wishes to thank the Czech Technical University, where this work was initiated, for hospitality and support.

References

1. R.A. Arndt, I.I. Strakovsky, and R.L. Workman, Phys. Rev. C **62** (2000) 034005; <http://gwdac.phys.gwu.edu>.
2. J. Ball *et al.*, Eur. Phys. J. C **5** (1998) 57.
3. J. Ball *et al.*, Eur. Phys. J. **11** (1999) 51.
4. A. de Lesquen *et al.*, Eur. Phys. J. **11** (1999) 69.
5. I. Pomeranchuk, Doklady Akad. Nauk **77** (1951) 249.
6. N.W. Dean, Phys. Rev. D **5** (1972) 1661; N.W. Dean, Phys. Rev. D **5** (1972) 2832.
7. V.I. Sharov *et al.*, Dubna report E1-2008-61 (2008).
8. J. Bystrický, F. Lehar, and P. Winternitz, J. Phys. (Paris) **39** (1978) 1.
9. D.V. Bugg and C. Wilkin, Nucl. Phys. A **467** (1987) 575.
10. J. Carbonell, M.B. Barbaro, and C. Wilkin, Nucl. Phys. A **529** (1991) 653.
11. R. de Tournell and D.W. Sprung, Nucl. Phys. A **201** (1973) 193.
12. N.B. Ladygina, Phys. Atom. Nucl. **71** (2007) 58.
13. R.J. Glauber, in *Lectures in Theoretical Physics*, ed. W.E. Brittin (Interscience, N.Y. 1959) vol. 1, p. 315.
14. V.K. Voitovetskii, I.L. Korsunskii, and Yu.F. Pazhin, Nucl. Phys. **69** (1965) 531.
15. W.M. Powell, UCRL report 1191 (1951).
16. D.F. Measday, Phys. Lett. **21** (1966) 66.
17. V.P. Dzhelepov, Proc. Int. Conf. High Energy Phys., Ed. J. Prentki, (CERN, Geneva, 1962) p. 19.
18. J.R. Cladis, J. Hadley, and W.N. Hess, Phys. Rev. **86** (1952) 110.
19. B. Pagels, Diplomarbeit : *Untersuchung der quasielastischen Ladungsaustauschreaktion $nd \rightarrow pnn$ im Neutronenergiebereich von 290 bis 570 MeV*, Universität Freiburg im Breisgau (1988).
20. V.P. Dzhelepov *et al.*, Izvestia Akad. Nauk **19** (1955) 573.
21. R.R. Larsen, Nuovo Cim. **18** (1960) 1039.
22. B.E. Bonner *et al.*, Phys. Rev. C **17** (1978) 664.
23. C. Wong *et al.*, Phys. Rev. **116** (1959) 104.
24. C.J. Batty, R.S. Gilmore and G.H. Stafford, Phys. Lett. **16** (1965) 137; A.S. Clough *et al.*, Nucl. Phys. A **121** (1968) 689.
25. J.A. Hofmann and K. Strauch, Phys. Rev. **90** (1953) 559.
26. A. Langsford *et al.*, Nucl. Phys. A **99** (1967) 246.
27. M.J. Esten, T.C. Griffith, G.J. Lush, A.J. Metheringham, Rev. Mod. Phys. **37** (1965) 533.
28. C.W. Bjork *et al.*, Phys. Lett. **63B** (1976) 31.
29. B.S. Aladashvili *et al.*, Nucl. Phys. B **86** (1975) 461.
30. V.V. Glagolev *et al.*, Eur. Phys. J. A **15** (2002) 471; *idem* Dubna report P1-2006-112 (2006).
31. C. Ellegaard *et al.*, Phys. Rev. Lett. **59** (1987) 974; T. Sams *et al.*, Phys. Rev. C **51** (1995) 1945.
32. S. Kox *et al.*, Nucl. Phys. A **556** (1993) 621.
33. D. Chiladze *et al.*, Phys. Lett. B **637** (2006) 170.
34. M.B. Barbaro and C. Wilkin, J. Phys. G **15** (1989) L69.
35. A. Kacharava, F. Rathmann, and C. Wilkin, COSY Proposal #152, *Spin Physics from COSY to FAIR*, [arXiv:nuc1-ex:0511028](https://arxiv.org/abs/nuc1-ex:0511028).